Electronic supplementary information
for
Enhanced photocatalytic activity of octahedral anatase particles prepared by hydrothermal reaction

Z. Wei[a], E. Kowalska[a*], K. Wang[a], C. Colbeau-Justin[b], B. Ohtani[a]

[a] Institute for Catalysis, Hokkaido University, N21, W10, 001-0021 Sapporo, Japan

[b] Laboratoire de Chimie Physique, CNRS UMR 8000, Université Paris-Saclay, Bat. 349, 91405 Orsay, France

*Corresponding author. Tel.: +81-11-706-9130 (kowalska@cat.hokudai.ac.jp)

Definition of morphology

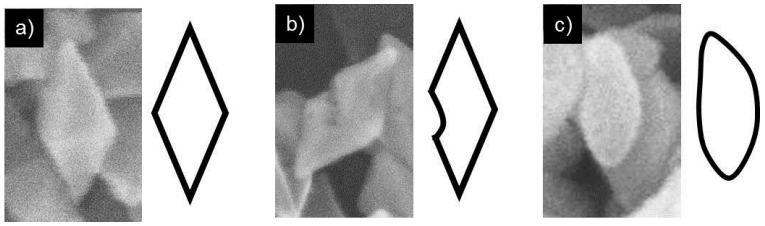

Fig. S1. Representative SEM images with respective models of a) OAPs, b) semi-OAPs and c) others [1].

Characterization of samples

The morphology of samples was studied by scanning electron microscopy (SEM, JEOL JSM-7400F), scanning transmission electron microscopy (STEM, HITACHI HD-2000) and transmission electron microscopy (TEM, JEOL JEM-2100F). The sample was dispersed in ethanol in an ultrasonic bath for a few seconds, and the suspension droplets were deposited on a carbon-covered copper microgrid, then it was vacuum dried overnight before the STEM and TEM tests. For SEM measurements, small amount of sample was adhered on the carbon paint covering copper specimen mount, then it was vacuum dried overnight before the test. Particles were classified into three groups based on SEM analysis: (1) OAP: an octahedral particle, (2) semi-OAP: an octahedral particle with a defect, and (3) others: irregularly shaped non-octahedral particle (Fig. S1). The content of these particles was measured by calculating more than 200 particles in several SEM images of each sample. Our previous study showed that the behaviors of OAPs and semi-OAPs were similar [1], and therefore for simplification total OAP content, i.e., the sum of both kinds of particles (1 and 2), is used in this paper.

XRD analysis was performed using the Rigaku intelligent X-ray diffraction system SmartLab equipped with a sealed tube X-ray generator (Cu target). Crystallite size was estimated from the corrected width of an anatase 101 diffraction peak using the Scherrer equation. Aspect ratio was calculated from the ratio of crystalline sizes estimated from the widths of diffraction peaks of (004) and (101). Crystallinity was evaluated using highly crystalline nickel oxide as an internal standard. Experimental details were presented in previous paper [2].

The oxidation states of elements and surface composition of samples were measured by XPS on JEOL JPC-9010MC (MgKα X-ray) spectrometer. Few milligram of sample was pasted on the surface of double-sided adhesive tape which was attached on the specimen stage. 50 scans were carried out for each element and the average data were taken for determination of titanium, oxygen and carbon.

Charge-carrier dynamics was studied by measuring time-resolved microwave conductivity (TRMC) induced by ns-timescale laser pulse at 355 nm. The incident microwaves were generated by a Gunn diode of the Kα band at 30 GHz. The pulsed light source was an OPO laser (EKSPLA, NT342B) tunable from 225 to 2000 nm. It delivers 8-ns FWMH pulses with a frequency of 10 Hz. The density of light energy received by the sample was 747 $\mu J.cm^{-2}$ at 355 nm.

Platinum particle-size distribution was determined by calculation of 154 and 248 NPs for samples prepared in the absence of oxygen (15-min Ar pre-bubbling) and in the presence of oxygen (15-min O_2 pre-bubbling), respectively. The obtained results are shown in Fig. 5(c).

Photocatalytic activity test

Photocatalytic activities of samples were evaluated for (a) acetic acid decomposition under aerobic conditions (CO_2 system) and (b) methanol dehydrogenation under deaerated conditions (H_2 system). A sample of photocatalyst was weighted (50 mg) into a borosilicate glass test tube (18 mm in diameter and 180 mm in length; transmits at > 290 nm) with a Teflon-coated magnet bar, to which 5.0-mL portion of (a) aqueous acetic acid (5vol%) or (b) aqueous methanol (50%) containing hexachloroplatinic acid (H_2PtCl_6; corresponding to 2wt% to a photocatalyst) was added. After argon bubbling to remove oxygen (for H_2 system) or without any bubbling (for CO_2 system), the tube was sealed off with a rubber septum and irradiated by a 400-W mercury arc (Eiko-sha) under vigorous magnetic stirring (1000 rpm) in a thermostated water bath (298 K). A portion of a gas phase (typically 0.1 mL from ca. 30-mL head space) was taken by a syringe and analyzed by gas chromatography (Shimadzu GC-8A gas chromatograph equipped with a thermal conductivity detector (TCD)) for (a) carbon dioxide (CO_2) and (b) hydrogen (H_2). The carrier gas was argon with flow rate of 40 mL min^{-1}. Stainless steel columns (3 mm in inner diameter) filled with Porapak Q (3 m) and molecular sieve 5A (3 m) were used for CO_2 and H_2. Since the pressure (atmospheric before photoirradiation) is increased with gas liberation, the amount of evolved gas was corrected for this pressure change.

In CO_2 system, only CO_2 liberation was detected by photoirradiation since acidity (acid strength) of acetic acid is higher than carbonic acid. The reaction stoichiometry has been confirmed for titania photocatalysts to be [3]:

$$CH_3COOH + 2O_2 \rightarrow 2CO_2 + 2H_2O$$

In general, time course of CO_2 liberation is almost linear without induction period and the slope of linear increase was calculated to be photocatalytic activity (in the unit of μmol h^{-1}).

In H_2 system, only H_2 liberation was detected by photoirradiation. Since the solubility of H_2 in water is negligible, it is possible to take H_2 amount in gas phase as liberated H_2 amount. The reaction stoichiometry has been confirmed to be [4, 5]:

$$CH_3OH \rightarrow HCHO + H_2$$

at least in the initial part of reaction where negligible liberation of CO_2 is observed, i.e., the following stoichiometry can be neglected.

$$CH_3OH + H_2O \rightarrow CO_2 + 3H_2$$

Since the H_2 liberation is negligibly slow in the absence of H_2PtCl_6, in-situ deposition of platinum on the surface of a photocatalyst is needed for this dehydrogenation. Stoichiometry of in-situ platinum deposition is considered to be [5, 6]:

$$H_2PtCl_6 + 2CH_3OH \rightarrow 2HCHO + Pt + 6HCl,$$

i.e., photoexcited electrons and positive holes are used for hexachloroplatinic acid reduction and

methanol oxidation, respectively. Then deposited platinum catalyzes the hydrogen evolution by capturing photoexcited electrons. The in-situ deposition is actually very fast and thereby time course of H_2 liberation exhibits, in general, no induction period for the deposition. Slope of H_2 increase (in the unit of μmol h^{-1}) was calculated to be photocatalytic activity.

For both CO_2 and H_2 systems, Showa Denko Ceramics FP-6 was used as a reference, since FP-6 is one of the most active photocatalysts for those reactions among many commercially available or non-profitably provided titania samples [7]. Actual rate of CO_2 and H_2 liberations by FP-6 in CO_2 and H_2 systems, respectively, were 39 and 540 μmol h^{-1} [2]. The reproducibility of photocatalytic activity tests was > 95%. In the present paper, activity of samples was shown as relative rate in reference to the above-mentioned rate for FP-6. Therefore, if the relative activity exceeded 100%, the sample exhibited the photocatalytic activity higher than commercially available or non-profitably provided titania samples.

In-situ platinum deposition by two methods

To prepare smaller platinum NPs, Pt was also deposited for oxygen-saturated suspension (15-min pre-bubbling), where photogenerated electrons were firstly consumed by oxygen, hindering formation of platinum aggregates. Rate of hydrogen evolution during methanol dehydrogenation for two methods (Ar or O_2 pre-bubbling) is shown in Fig. S2. It is clear that under anaerobic conditions (Ar pre-bubbling) hydrogen is evolved immediately when irradiation started (without induction period). Lack of induction period and the constant reaction rate during whole irradiation duration indicate that platinum NPs are formed during first seconds of irradiation. In contrary, under aerobic conditions (O_2 pre-bubbling), during first two hours of irradiation hydrogen is not formed and photogenerated electrons are scavenged by oxygen. After 150 min of irradiation, with increase in oxygen consumption, platinum NPs are slowly formed and hydrogen is evolved. Then, the linear evolution of hydrogen is observed at ca. 270 min of irradiation suggesting that all platinum cations have been reduced and formation of platinum NPs has been finished.

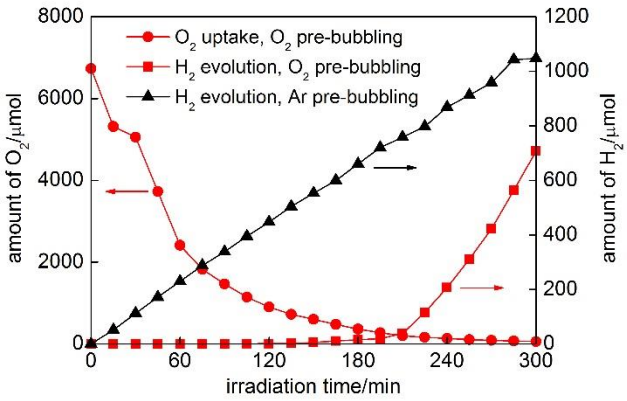

Fig. S2. In-situ platinum photodeposition from deaerated (15-min Ar pre-bubbling) and aerated (15-min O_2 pre-bubbling) suspensions of methanol.

Influence of TNWs concentration on properties of titania

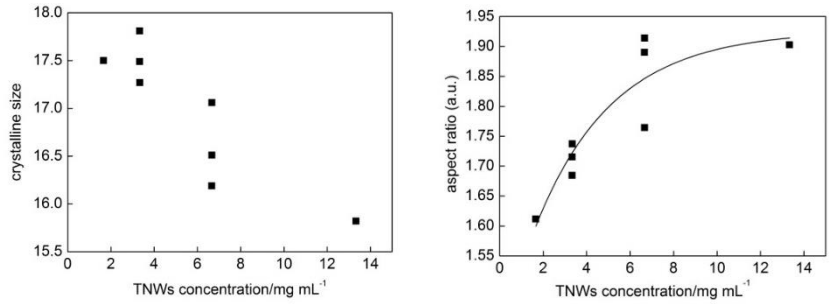

Fig. S3. Influence of TNW concentration on (left) crystalline size and (right) on aspect ratio.

Properties of samples

Table S1 Structural/physical properties and photocatalytic activities of samples prepared from various conditions (optimization group)

no.	Code	TNWs /mg	Milli-Q water/ mL	Concent-ration /g mL^{-1}	Size /nm	As-pect ratio	Total OAP content (%)	CO_2 (%)	H_2 (%)	I_{max} /V	I_{40ns} /I_{max}	I_{4000ns} /I_{max}
1	100/30	100	30	3.33	17.8	1.68	50	87	4	0.136	0.819	0.215
2	200/30	200	30	6.66	17.0	1.76	45	74	39	0.253	0.841	0.184
3	200/60	200	60	3.33	17.5	1.72	53	97	38	0.209	0.787	0.182
4	400/60	400	60	6.66	16.5	1.91	48	87	30	0.357	0.837	0.183
5	133/80	133	80	1.66	17.5	1.61	49	98	39	0.138	0.899	0.451
6	267/80	267	80	3.33	17.2	1.71	64	145	37	0.258	0.893	0.352
7	533/80	533	80	6.66	16.2	1.89	41	74	33	0.468	0.821	0.170
8	1067/80	1067	80	13.33	15.8	1.90	46	92	29	0.607	0.884	0.289

XPS results

To characterize surface composition of the samples, oxygen, titanium and carbon were analyzed by XPS method and obtained data are summarized in Table S2.

It was found that ratio of oxygen to titanium exceeded those of chemical titania formula (O:Ti = 2) reaching ca. four, which is not surprised since usually titania samples possess excess of oxygen on the surface, depending on preparation method. For example, ratio of 4.6 was reported for titania samples prepared by microemulsion method [8]. Deficiency of oxygen has also been found, especially in the case of synthesis performed in the lack of sufficient amount of oxygen [9]. Adsorbed carbon dioxide could be also one of the sources of surface oxygen as C/Ti ratios correlate with O/Ti ratios, i.e., the larger content of carbon is, the larger is the content of oxygen in the samples. In present study, the lowest O:Ti ratio of ca. 3.0 was obtained for two samples, 200/60 and 533/80. Interesting it was found that for constant volume, O:Ti ratio increased with increase of TNWs content (except for 533/80 sample), which could be caused by larger amount of hydroxyl groups as a result of KOH formation during HT process (reaction shown in 3.2.).

Table S2 XPS analysis of the samples prepared from various conditions

Group	no.	Code	Ti (%)	O (%)	C (%)	O/Ti	C/Ti	O 1s (%)			C 1s (%)		
								TiO_2	Ti-(OH)-Ti/Ti_2O_3/C=0	Ti-OH/C-OH	C-C	C-OH	C=O
Optimization group	1	100/30	8.82	32.2	58.98	3.7	6.7	42.02	33.02	24.96	67.39	22.95	9.66
	2	200/30	6.35	27.99	65.67	4.4	10.3	34.96	33.97	31.07	65.97	23.96	10.07
	3	200/60	10.51	31.62	57.88	3.0	5.5	50.12	32.14	17.74	67.04	24	8.96
	4	400/60	6.73	29.4	63.87	4.4	9.5	30.81	33.94	35.25	66.35	24.08	9.57
	5	133/80	8.28	28.77	62.95	3.5	7.6	42.16	34.59	23.25	63.02	28.04	8.94
	6	267/80	7.39	28.64	63.97	3.9	8.7	39.4	32.53	28.07	63.67	27.13	9.2
	7	533/80	12.19	35.06	52.76	2.9	4.3	51.92	28.95	19.13	60.78	30.58	8.64
	8	1067/80	6.06	29.81	64.13	4.9	10.6	31.47	34.80	33.73	64.08	25.71	10.22
TNWs	9	TNWs	26.72	51.17	22.11	1.9	0.8	78.36	20.7	0.94	96.23	3.77	0

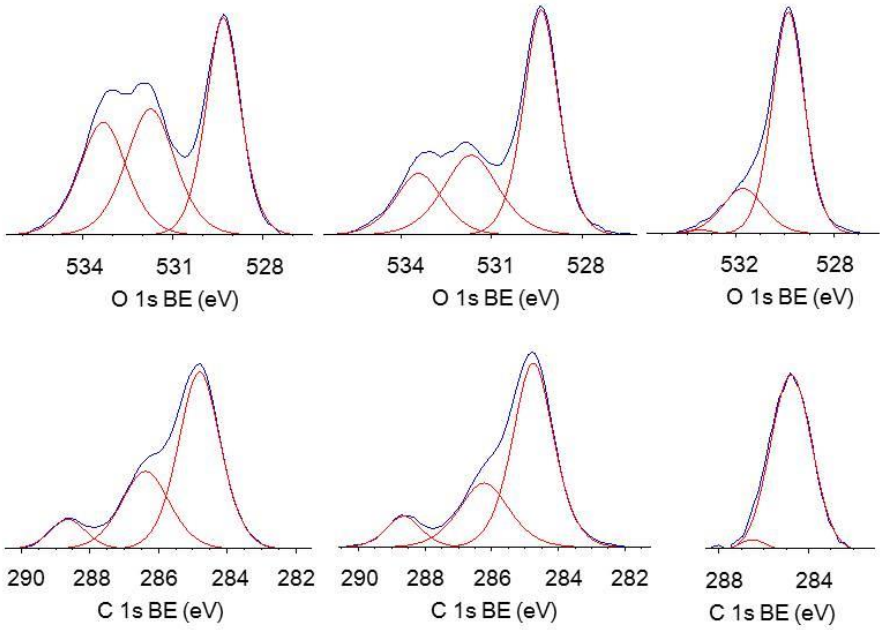

Fig. S4. XPS results for (top) O 1s and (down) C 1s of 533/80 sample (left), 267/80 sample (middle) and TNWs (right).

Moreover, the form of present oxygen also differed in particular samples, as exemplary shown in Fig. 4. According to literature reports, O 1s peak could be composed of three to five different species [10]. For example, in the form of Ti-O bonds in TiO_2 and Ti_2O_3, H-O bonds in hydroxyl groups, carbon bonds (C-O and C=O) and adsorbed water. In our study, three peaks were observed in all samples at binding energy (BE) of ca. 529.5, 531.7 and 533.3 eV, respectively, as exemplary shown in Fig. S4. The first peak was related to oxygen in the crystal lattice of titania (TiO_2), the second peak to C=O, Ti_2O_3, and/or OH groups binding with two Ti atoms, while the third peak mainly to hydroxyl groups bound to titanium and carbon (Ti-OH, C-OH) [11]. Oxygen in the form of hydroxyl groups was predominant form in 267/80 sample, while it was mainly bounded (in TiO_2) in 533/80 sample. The similar dependence to O:Ti ratio was noticed, i.e., increase in content of hydroxyl groups with increase in TNWs amount. For comparison, 1s oxygen was also analyzed for TNWs and presented in the right part of Fig. S4. Although main content of oxygen was in the

bounded form of TNWs structures (78%), small amount of oxygen in the form of either hydroxyl groups or C=O was also noticed. However, the amount of bounded hydroxyl groups was negligible reaching less than 1%. Titanium was mainly present in the form of Ti^{+4} at BE of 458.0-458.1 eV, and only three samples prepared with largest volume (133/80, 267/80 and 533/80) contained slight amount of Ti^{+3} (BE=456.3 eV) of less than 3%. Similarly, forms of carbon practically did not differ between the samples. Carbon 1s region was deconvoluted for three peaks at BE of 284.7, 286.3 and 288.6 eV, which could be assigned to C-C, C-OH and C=O states [10, 12], and obtained amounts were 61-67%, 23-31% and 9-10% respectively.

Dependences of photocatalytic activities on properties of samples:

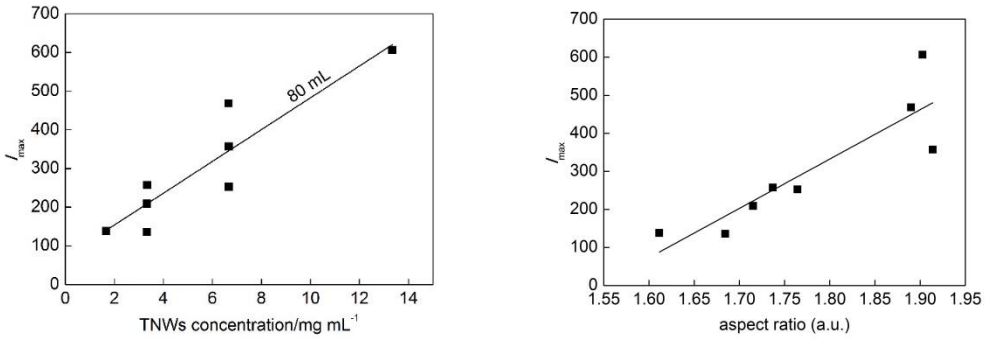

Fig. S5. Influence of (left) TNWs concentration and aspect ratio (right) on I_{max}.

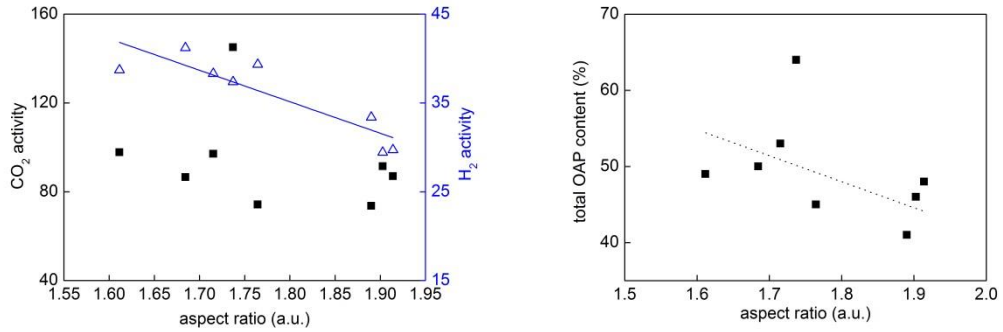

Fig. S6. Influence of aspect ratio on (left) photocatalytic activity and (right) total OAP content.

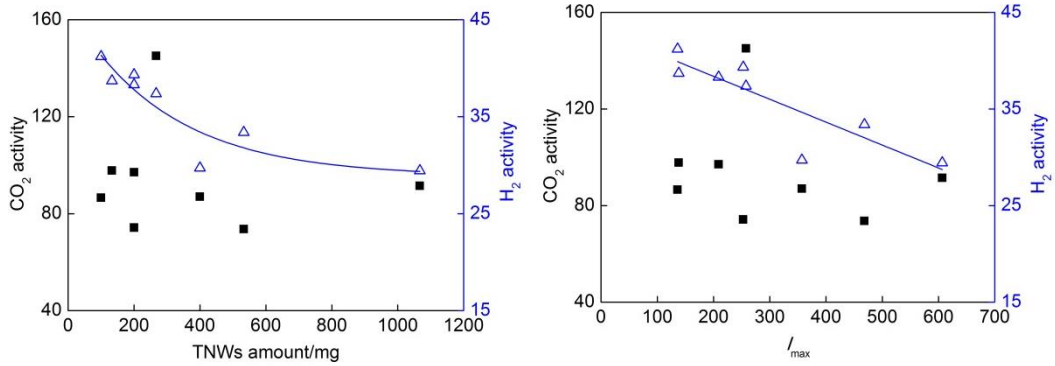

Fig. S7. Influence of TNWs amount (left) and I_{max} (right) on photocatalytic activity.

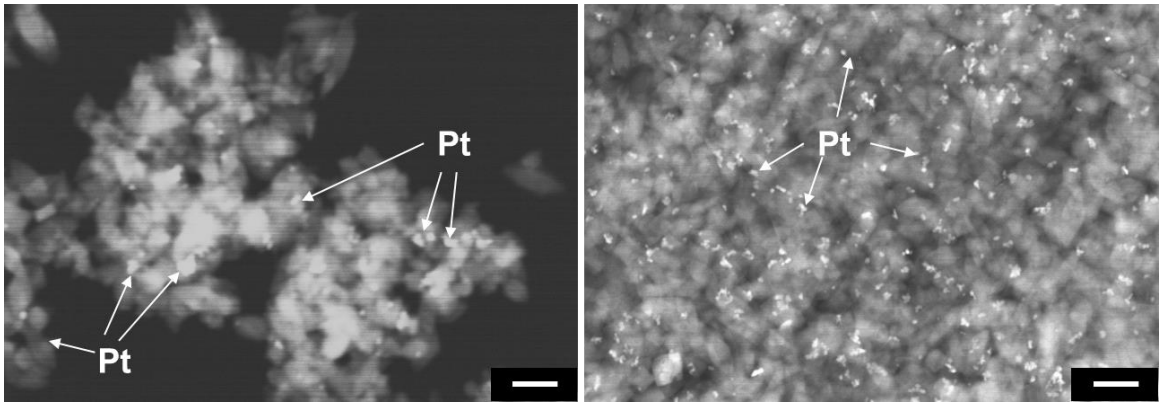

Fig. S8. STEM images of Pt/OAP prepared by two photodeposition methods: after bubbling with argon (left) and oxygen (right): Scale bars correspond to 50 nm.

Influence of pH value

Table S3 Structural/physical properties and photocatalytic activities of sample containing OAPs prepared from different pH.

no.	Code	TNWs /mg	pH of sus-pen-sion	Milli-Q water/ mL	Concen-tration /g mL-1	Size /nm	Aspect ratio	Total OAP content (%)	CO_2 (%)	H_2 (%)	I_{max} /mV	I_{40ns} /I_{max}	I_{4000ns} /I_{max}
1	pH3	267	3	80	3.33	15	1.50	38	105	37	0.136	0.787	0.180
2	pH6	267	6	80	3.33	17.21	1.71	64	145	37	0.258	0.893	0.352
3	pH11	267	11	80	3.33	15.8	2.00	3	46	9	0.168	0.715	0.043

References:

[1] Z. Wei, E. Kowalska, J. Verrett, C. Colbeau-Justin, H. Remita, B. Ohtani, Nanoscale 7 (2015) 12392-12404.

[2] Z. Wei, E. Kowalska, B. Ohtani, Molecules 19 (2014) 19573-19587.

[3] H. Kominami, J.I. Kato, M. Kohno, Y. Kera, B. Ohtani, Chem. Lett. (1996) 1051-1052.

[4] S.I. Nishimoto, B. Ohtani, T. Kagiya, J. Chem. Soc. Farad. Trans. 181 (1985) 2467-2474.

[5] H. Kominami, T. Matsuura, K. Iwai, B. Ohtani, S. Nishimoto, Y. Kera, Chem Lett (1995) 693-694.

[6] B. Ohtani, K. Iwai, S.-i. Nishimoto, S. Sato, J. Phys. Chem. B 101 (1997) 3349-3359.

[7] B. Ohtani, O.O.P. Mahaney, F. Amano, N. Murakami, R. Abe, J. Adv. Oxid. Technol. 13 (2010) 247-261.

[8] A. Zielińska-Jurek, E. Kowalska, J.W. Sobczak, W. Lisowski, B. Ohtani, A. Zaleska, Appl. Catal. B: Environ. 101 (2011) 504-514.

[9] J. Reszczynska, T. Grzyb, Z.S. Wei, M. Klein, E. Kowalska, B. Ohtani, A. Zaleska-Medynska, Appl. Catal. B-Environ. 181 (2016) 825-837.

[10] J.G. Yu, X.J. Zhao, Q.N. Zhao, Thin Solid Films 379 (2000) 7-14.

[11] J. Reszczynska, T. Grzyb, J.W. Sobczak, W. Lisowski, M. Gazda, B. Ohtani, A. Zaleska, Appl. Surf. Sci. 307 (2014) 333-345.

[12] J. Reszczynska, T. Grzyb, J.W. Sobczak, W. Lisowski, M. Gazda, B. Ohtani, A. Zaleska, Appl Catal B-Environ 163 (2015) 40-49.